

## Case Report



# The application of “bone window technique” using piezoelectric saws and a CAD/CAM-guided surgical stent in endodontic microsurgery on a mandibular molar case

Ukseong Kim ,<sup>1</sup> Sunil Kim ,<sup>1</sup> Euseong Kim <sup>1,2\*</sup>

<sup>1</sup>Microscope Center, Department of Conservative Dentistry and Oral Science Research Center, Yonsei University College of Dentistry, Seoul, Korea

<sup>2</sup>Department of Electrical & Electronic Engineering, Yonsei University College of Engineering, Seoul, Korea



Received: Dec 2, 2019

Revised: Feb 25, 2020

Accepted: Feb 25, 2020

Kim U, Kim S, Kim E

### \*Correspondence to

Euseong Kim, DDS, MSD, PhD

Professor, Microscope Center, Department of Conservative Dentistry and Oral Science Research Center, Yonsei University College of Dentistry, 50-1 Yonsei-ro, Seodaemun-gu, Seoul 03722, Korea.  
E-mail: andyendo@yuhs.ac

Copyright © 2020. The Korean Academy of Conservative Dentistry

This is an Open Access article distributed under the terms of the Creative Commons Attribution Non-Commercial License (<https://creativecommons.org/licenses/by-nc/4.0/>) which permits unrestricted non-commercial use, distribution, and reproduction in any medium, provided the original work is properly cited.

### Funding

This work was supported by the Basic Science Research Program through the National Research Foundation of Korea (NRF) funded by the Ministry of Education (grant No. 2018R1D1A1A09081906).

### Conflict of Interest

No potential conflict of interest relevant to this article was reported.

## ABSTRACT

Apical surgery for a mandibular molar is still challenging for many reasons. This report describes the applications of computer-guided cortical ‘bone-window technique’ using piezoelectric saws that prevented any nerve damage in performing endodontic microsurgery of a mandibular molar. A 49-year-old woman presented with gumboil on tooth #36 (previously endodontically treated tooth) and was diagnosed with chronic apical abscess. Periapical lesions were confirmed using cone-beam computed tomography (CBCT). Endodontic microsurgery for the mesial and distal roots of tooth #36 was planned. Following the transfer of data of the CBCT images and the scanned cast to an implant surgical planning program, data from both devices were merged. A surgical stent was designed, on the superimposed three-dimensional model, to guide the preparation of a cortical window on the buccal side of tooth #36. Endodontic microsurgery was performed with a printed surgical template. Minimal osteotomy was required and preservation of the buccal cortical plate rendered this endodontic surgery less traumatic. No postoperative complications such as mental nerve damage were reported. Window technique guided by a computer-aided design/computer-aided manufacture based surgical template can be considerably useful in endodontic microsurgery in complicated cases.



**Keywords:** Endodontic microsurgery; Bone window; Surgical guide; Computer-aided design/Computer-aided manufacturing; Piezoelectric surgery

## INTRODUCTION

Endodontic microsurgery is the treatment option frequently opted to manage endodontically failed cases with persistent apical periodontitis, after nonsurgical root canal treatment [1,2]. The success rate of conventional apical surgery is relatively low, ranging between 43.5% and 74% [3]. However, the application of current techniques, including magnification and illumination provided by the microscope, new microsurgical instruments, and new root-end filling materials [4], have improved the success rates of endodontic surgery remarkably, and subsequently, surgical retreatment has become an effective treatment option for cases

**Author Contributions**

Conceptualization: Kim E; Data curation: Kim U; Funding acquisition: Kim E; Investigation: Kim S; Methodology: Kim E; Project administration: Kim E; Resources: Kim E; Software: Kim U; Supervision: Kim S, Kim E; Validation: Kim S; Visualization: Kim U; Writing - original draft: Kim U; Writing - review & editing: Kim S, Kim E.

**ORCID iDs**Ukseong Kim <https://orcid.org/0000-0002-5101-8767>Sunil Kim <https://orcid.org/0000-0002-8889-9844>Euseong Kim <https://orcid.org/0000-0003-2126-4761>

non-responsive to non-surgical endodontic treatment. Success rates of modern endodontic microsurgery have been reported between 88.9% and 100% [3].

The outcomes of endodontic microsurgery are affected by several prognostic factors including lesion type, retrograde filling material, and coronal restoration [5]. Several studies have reported the effect of tooth position on the surgical outcome. Especially, mandibular molars showed poorer success rates than teeth in other positions. Difficulties in achieving adequate accessibility owing to the thickness of cortical bone on the buccal side and additional anatomic impediment, including the inferior alveolar nerve or the mental foramen, have been attributed to poorer outcomes [6,7].

The extent of periapical bone defect is another factor known to affect healing [8]. The degree of postoperative complications, including pain and swelling, is influenced by the amount of osteotomy [9]. Traditional osteotomy methods utilize large round burs. With traditional methods, a significant amount of cortical bone loss is inevitable. Increased postoperative pain, delayed healing, and other complications such as nerve damage are frequently associated with these methods [4]. Otherwise, piezo-surgical devices allow accurate resection of mineralized tissues while the surrounding soft tissues, such as nerves, blood vessels, and mucosa remains uninjured. In contrast, the traditional method of crypt creation is free-hand guided, which can damage the surrounding soft tissues.

The ‘bone window’ approach to the apical region is a less invasive and less traumatic procedure that minimizes bone loss in comparison to the traditional osteotomy techniques. Cone-beam computed tomography (CBCT) and computer-aided design/computer-aided manufacture (CAD/CAM) can determine the three-dimensional (3D) extent of the required cortical window. Surgical templates, printed from 3D imaging data, optimize site preparation, determine the dimensions of the osteotomy as well as the extent of the pathology [10,11]. Such 3D-printed stereolithographic surgical templates can guide the osteotomies during surgeries, minimizing deviation from the digitally established surgical plans.

In this report, we present a safe, less traumatic, and more convenient method of endodontic microsurgery involving the application of “bone window technique” using a piezo-surgical device and a CAD/CAM based surgical template.

## CASE REPORT

A 49 years old woman was referred from the department of periodontology due to the presence of a sinus tract on tooth #36 (**Figure 1A**). She did not report any discomfort associated with the tooth. The medical history was non-contributory. However, periapical radiographs with gutta-percha tracing revealed periapical radiolucent lesions associated with both mesial and distal roots of tooth #36, and the origin of the sinus tract was the distal root of tooth #36 (**Figure 1B**). Periodontal probing depths were unremarkable. In her dental history, she reported that tooth #36 was endodontically treated 2 years previously. Apical lesions were confirmed by CBCT images (Alphrad 3030, Asahi Roentgen Ind Ltd., Kyoto, Japan). Based on the history and clinical and radiographic examination, a diagnosis of a previous root canal treatment with chronic apical abscess was established. A decision to perform endodontic microsurgery on both mesial and distal roots of tooth #36 was made. The patient was offered all treatment options; she opted for endodontic microsurgery.

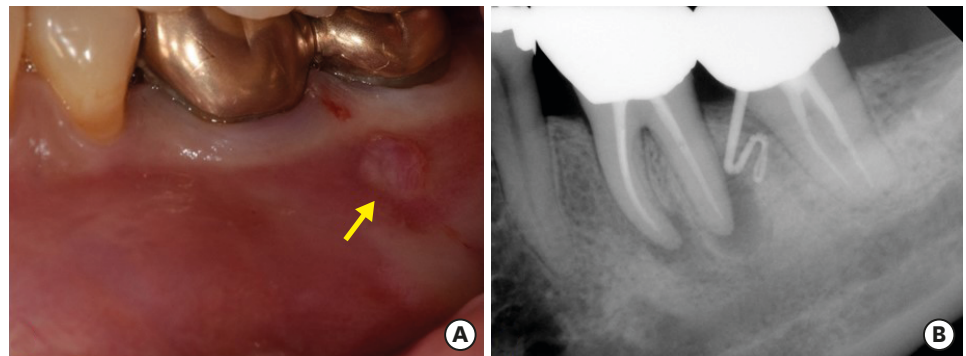


**Figure 1.** (A) The clinical image of tooth #36 with the sinus tract on buccal gingiva (yellow arrow). (B) The initial periapical radiograph of tooth #36 showing periapical lesions and gutta percha tracing revealing the origin of the sinus tract was the distal root of tooth #36.

Written consent was obtained. The exact localization of the apex of the 2 roots was expected to be difficult due to the presence of thick buccal cortical bone, especially close to the tip of the distal root and the inter-radicular area. Further, substantial loss of buccal cortical plate was anticipated with the traditional osteotomy technique using round burs. Therefore, cortical window access using a surgical template was planned.

A preliminary impression was obtained using irreversible hydrocolloid. Based on the obtained preliminary impressions, the diagnostic cast was fabricated using type III gypsum product. The diagnostic casts were scanned using a 3D scanner (Identica Blue, Medit, Seoul, Korea).

The CBCT images of the tooth and the data obtained from the scanned casts were uploaded to dental CAD software (Exocad GmbH; Darmstadt, Germany) and superimposed (**Figure 2A-2C**). The coronal portion of the scanned casts above the marginal gingiva and the radicular portion of the CBCT images of the tooth were selected and merged (**Figure 2D**). Occlusal indentations for the surgical stent were obtained from the coronal portion of the scanned cast, and the geometry of the bony structures was determined from the CBCT images. A surgical stent was designed using this merged data (**Figure 2E**). An indentation was made on the design of the stent using the erase brush tool for obtaining a rectangular-shaped window over the apical lesions. The extent of the window was designed to include both mesial and distal apical lesions, and confirmed by referring to the superimposed CBCT images (**Figure 2F**).

The designed surgical template was exported in a stereolithography file format. This file was printed using a photopolymer printer (Object EDEN260V, Stratasys, Eden Prairie, MN, USA). Biocompatible clear resin (MED610, Stratasys), approved in accordance with standard DIN EN ISO 10993-1:2009, was used for printing. After completion of the printing process, the surgical window was prepared with the rectangular indentation as a guide, using a denture bur (**Figure 2G and 2H**).

All surgical procedures were performed under a dental operating microscope (OPMI PICO, Carl Zeiss, Göttingen, Germany). On the day of surgery, the fit of the 3D-printed surgical template was verified intraorally. The patient was anesthetized using 2% lidocaine with 1:80,000 epinephrine followed by sulcular full-thickness flap reflection using tissue elevators. After flap reflection, the mental neurovascular bundle was identified, and a groove was formed just above using the piezoelectric surgery unit (Piezotome M+, Acteon, Mérignac, France) with fine-toothed saw tips (BS1S). A KP1 retractor (G Hartzell and Son

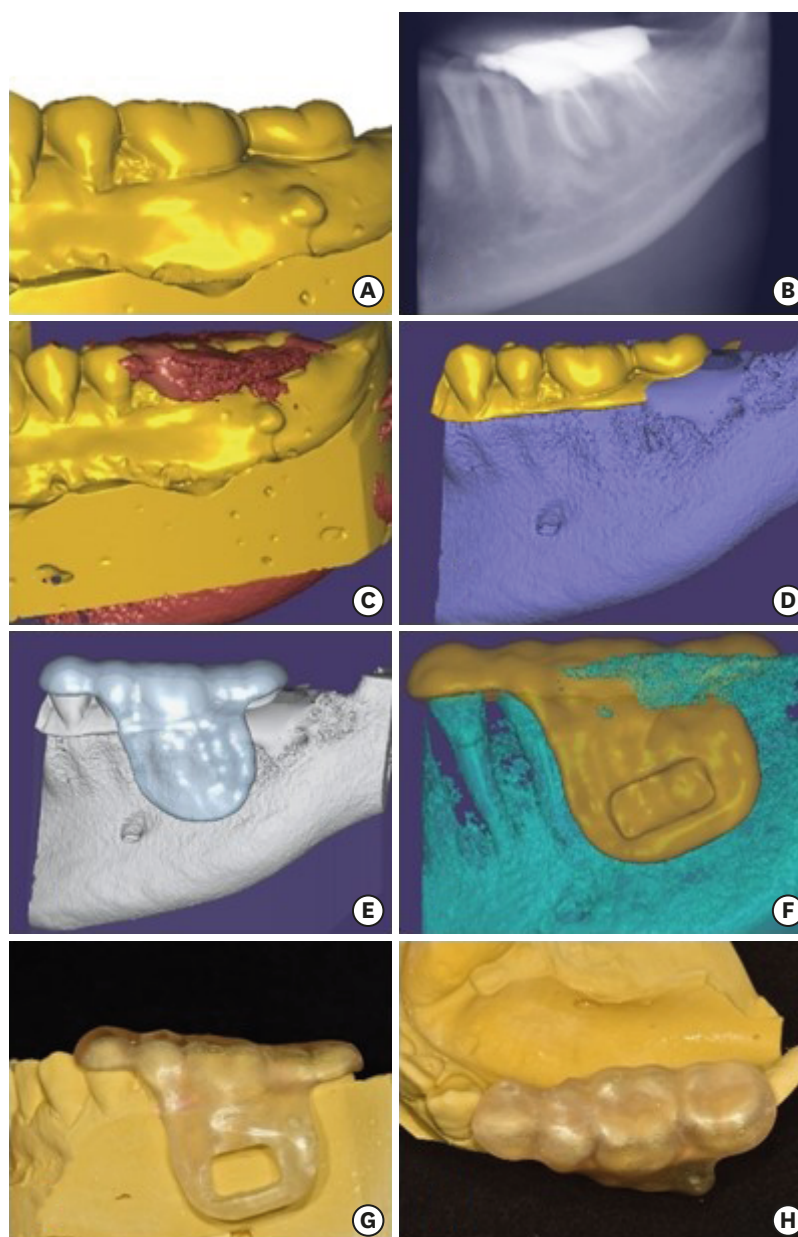


**Figure 2.** (A) Scanning data of the cast. (B) Cone-beam computed tomography (CBCT) image of the tooth uploaded to the surgical planning software. (C) Superimposition of the scanned cast and the CBCT image. (D) The coronal portion of the scanned cast above the level of the marginal gingiva and the gingival portion of the CBCT data were selected and merged. (E) The initial design of the surgical template without window. (F) The final design of the surgical template with window. (G, H) The buccal and the occlusal view of the 3D printed surgical template for endodontic surgery on tooth #36.

Inc., Concord, CA, USA) was placed to protect the nerve. (**Figure 3A-3C**) The printed surgical guide was positioned on the predetermined position (**Figure 3D**), and guided osteotomy for the preparation of a cortical window was performed using piezoelectric saws (**Figure 3E** and **3F**). After the surgical template was removed, the cortical lid, obtained from osteotomy guided by the rectangular window, was removed and stored in Hank's balanced salt solution (Gibco, Grand Island, NY, USA) until the end of the surgical procedure. The uncovered lesion and the apices of the roots were examined (**Figure 3G**). Curettage was performed on

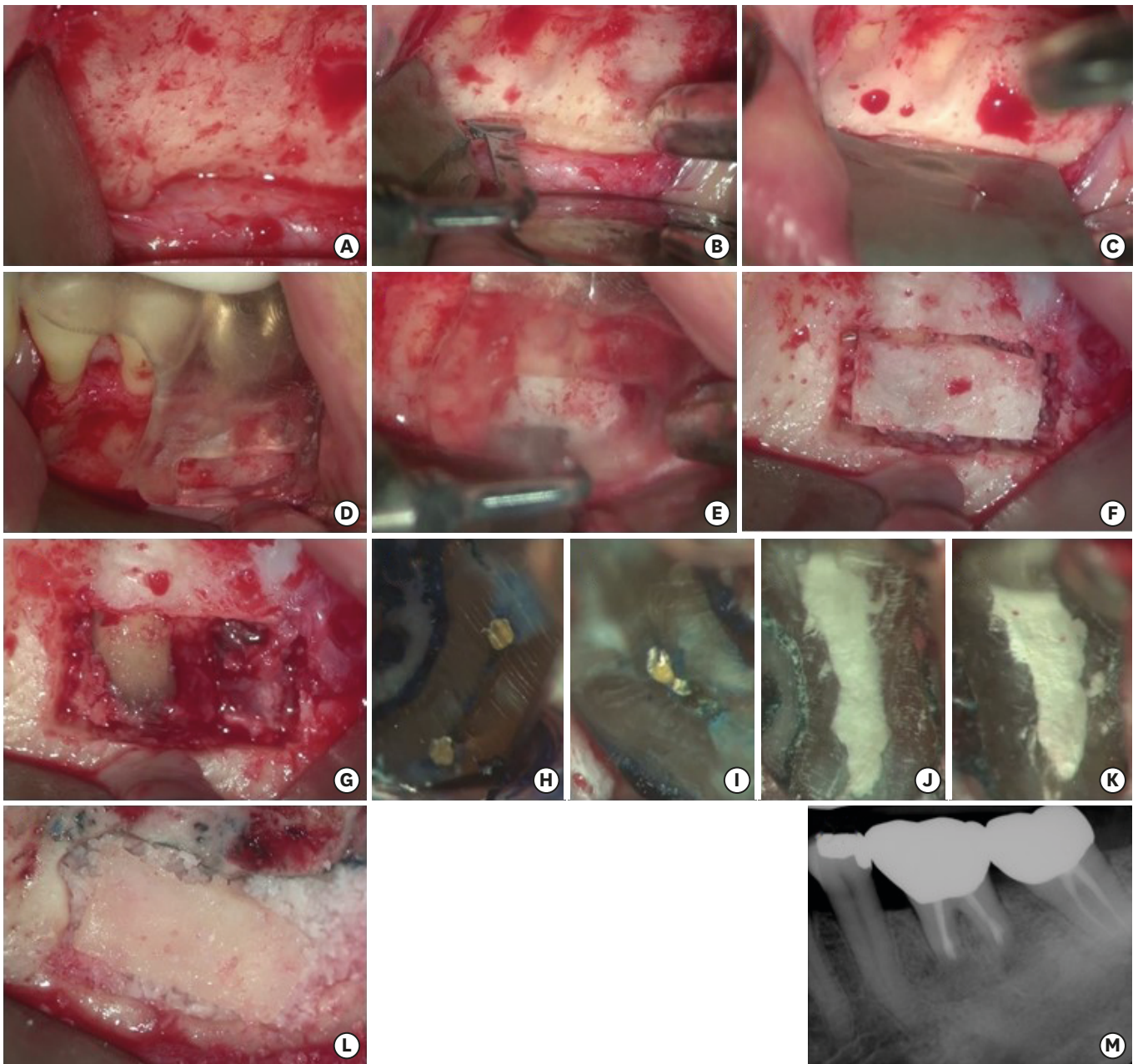


**Figure 3.** (A) After flap reflection, metal foramen and mental nerve was identified. (B) A groove was made using the piezoelectric saw on the coronal side of the mental foramen to protect it. (C) A KPI retractor was placed on the groove. (D) The surgical template was positioned on tooth #36. (E) Guided osteotomy for preparation of the cortical window was performed using piezoelectric saws. (F) Bone preparation for the cortical window. (G) Uncovered area of the lesion and the apices of the roots. (H) The resected root surface inspected under high magnification. An isthmus was observed on the mesial root. (I) The resected root surface inspected under high magnification. An isthmus was observed on the distal root. (J, K) Root-end filling with Retro MTA on the mesial root and the distal root were confirmed under high magnification. (L) Allogenic bone was grafted and cortical bone was repositioned. (M) The postoperative periapical radiograph.

periapical areas followed by 3 mm root tip resections using a 170-tapered fissure bur under copious irrigation with sterile distilled water. Cotton pellets, soaked in 0.1% epinephrine solution (Bosmin, Jeil Pharmaceutical Co, Ltd., Seoul, Korea), were placed in the bony crypt to achieve hemostasis. The resected root surfaces were stained with methylene blue, and inspected using a micromirror (Obtura Spartan, Fenton, MO, USA) with 20× to 26× magnification. An isthmus was observed between the canals in both mesial and distal roots

each. Isthmi were included in the root-end cavity preparation design (**Figure 3H** and **3I**). The root-end preparation was extended 3 mm into the canal space along the axis of the root using KIS ultrasonic tips (Obtura Spartan). The prepared root-end cavity was dried and retrograde root canal filling with mineral trioxide aggregate (retroMTA, BioMTA Co., Seoul, Korea) was completed. Adaptation of MTA to the canal was confirmed under high magnifying power (20×–26×) (**Figure 3J** and **3K**). After cleaning the surgical field, bone grafting was performed with allogenic bone (THE Graft, Purgo, Seongnam, Korea), and the stored cortical bone was repositioned on the grafted bone (**Figure 3L**). Because of the definite stability of the bony window, a membrane coverage over the grafted site was not performed and the flap was repositioned and sutured using 5-0 monofilament sutures. To verify the absence of excess material in the bony crypt, and an accurate extension of the root-end fillings, a postoperative radiograph was obtained (**Figure 3M**).

No postoperative complications were reported and the healing process was uneventful. The sutures were removed 7 days after the surgery. The patient presented for follow-up at 6 (**Figure 4A** and **4B**) and 12 (**Figure 4C**) months with radiographic signs of healing and no clinical signs or symptoms.

## DISCUSSION

The dimensions of a bony defect influence the postoperative condition of patient and healing after endodontic surgery. Excessive bone destruction can lead to unsuccessful, uncertain, or delayed healing [8,12], and an increased risk of postoperative complications. Especially, the height of the remaining buccal bone plate (*i.e.*, the apicocoronal distance of the buccal

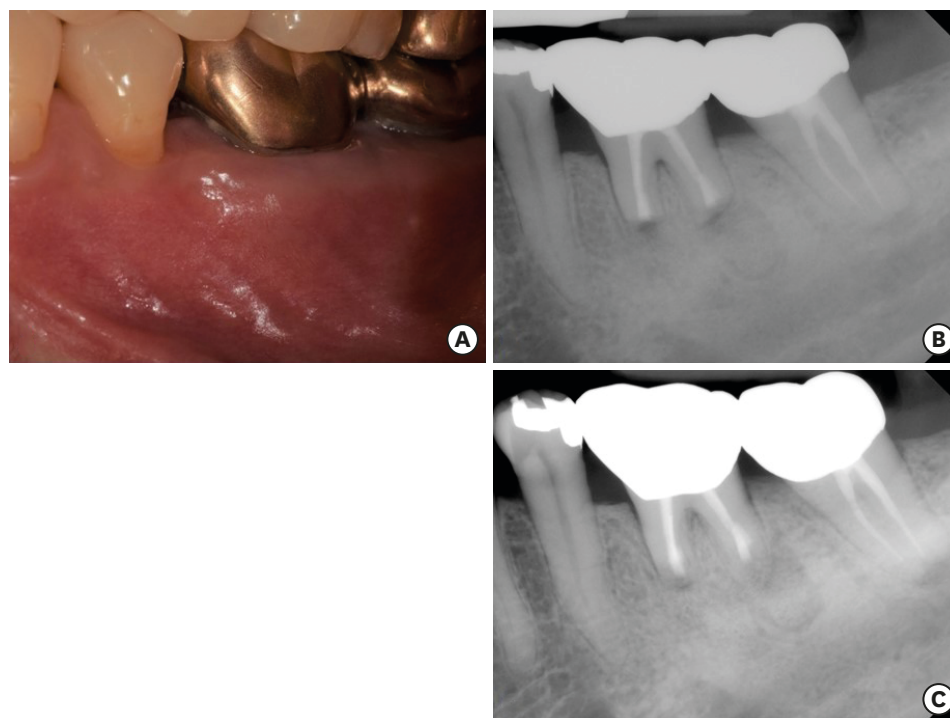


**Figure 4.** (A) The 6 months follow-up clinical image. (B) The 6 months follow-up periapical radiograph. (C) The 12 months follow-up periapical radiograph.

bone plate covering the root surface) was found to be associated with the healing outcome. Insufficient marginal bone caused by unintended extension of osteotomy would result in a lower success rate of surgery [12]. Excessive osteotomy can be occurred inadvertently in endodontic microsurgery cases, particularly in molar regions with apical lesion on a distal root because of difficulties in approach [13].

Surgical trauma was minimized in this case by the use of a 3D-printed surgical template for performing guided and minimal osteotomy, forming a surgical window over the area including both apical lesions. Further, after the completion of the surgical procedures, the stored cortical bone obtained from the window was repositioned to serve as an autogenous bone graft, which promoted early healing. Surgical damage, including osteotomy, initiates the inflammatory process, which leads to postoperative complications such as pain and swelling [9]. Surgical complications can be minimized and healing can be promoted by reducing the extent of the osteotomy. Therefore, the 'guided window' type of osteotomy using a 3D-printed surgical template can decrease postoperative complications and enhance healing.

Although it is a time-consuming process to make a CAD/CAM based surgical template [12], the surgical time can be decreased. As in this case, the fabrication of a surgical template helped in the precise preparation of a single bone window. The 2 root apices were visualized immediately after the removal step of the cortical window, and the need to search for root apices was obviated. In addition, the single large bone window provided better access for the enucleation of the diseased tissue, without any interruption. As the degree of postoperative swelling is influenced by the duration of the surgical procedure, strategies directed to reduce the duration of surgery should be utilized to reduce the post-operative discomfort of the patients [14].

Surgical templates are particularly useful in difficult cases involving teeth proximal to potentially critical anatomic structures. Structures such as the adjacent root tips, inferior alveolar nerve, mental foramen, and maxillary sinus pose significant difficulties in achieving adequate access to the root apex [10]. However, guided surgery performed using a customized surgical template can help in bypassing the critical anatomic landmarks. Hence, CAD/CAM-guided surgical templates can broaden the indications for endodontic microsurgery.

Fabrication of an accurate surgical template requires proper case selection and accurate design. Scatter in CBCT images, which originate from metallic restorations, can lead to inaccurate superimposition with scanned casts. Hence, the accuracy of surgical templates is limited in patients with several metallic prostheses and/or restorations [15]. In the present case as well, several prostheses created artifacts in the CBCT images (**Figure 2C**). However, the natural tooth (tooth #35) proximal to the surgical area made superimposition possible. Moreover, the coronal portion was selected from the scanned cast and the radicular portion with the alveolar bone was selected from the CBCT images. Using this method, the effects of the artifacts caused by the metallic prosthesis were neutralized and a well-fitting surgical guide was fabricated.

Piezoelectric instruments ensure precise and safe selective sectioning of the mineralized tissues such as bone and preserve the soft tissues such as blood vessels, nerves, and mucosa. Furthermore, the 'air-water cavitation effect' provides better visibility by creating a clear and blood-free surgical field [16]. With these properties, groove formation above the mental nerve and 'bone-window technique' can be performed safely, less traumatically, and more conveniently.

The use of a membrane in guided bone regeneration (GBR) procedure is thought to be advantageous, achieving mechanical stabilization and preventing ingrowth of surrounding soft tissue cells to a grafted site [17]. A few authors claimed that the use of membrane rather interferes with microvascular circulation leading to a delay in healing of mucoperiosteal flap [18]. However, some studies showed results that there is no difference in the use of a membrane. Yet other factors, such as proper healing period, healthy periosteum, and good oral hygiene, played important roles in bone regeneration after GBR [19]. In this case, the following factors lead to a satisfactory surgical outcome without the use of a membrane. The repositioned window bone over the grafted allogenic bone showed definite stability. Periosteal damage was minimized through giving clean incision and careful flap reflection. Primary closure was achieved without any relieving incisions.

## CONCLUSIONS

Within the limitations of this clinical case, using a CAD/CAM-guided surgical template and the window technique in endodontic surgery prevents the formation of large residual bone defects after endodontic microsurgery and the repositioned cortical bone obtained from the window can act autogenous bone graft, which promoted early healing. Additionally, introducing a CAD/CAM-guided surgical template and piezoelectric saws enable a surgeon to perform surgery as planned safely, less traumatically, and conveniently.

## REFERENCES

1. Kang M, Jung HI, Song M, Kim SY, Kim HC, Kim E. Outcome of nonsurgical retreatment and endodontic microsurgery: a meta-analysis. *Clin Oral Investig* 2015;19:569-582.  
[PUBMED](#) | [CROSSREF](#)
2. Gorni FG, Gagliani MM. The outcome of endodontic retreatment: a 2-yr follow-up. *J Endod* 2004;30:1-4.  
[PUBMED](#) | [CROSSREF](#)
3. Setzer FC, Shah SB, Kohli MR, Karabucak B, Kim S. Outcome of endodontic surgery: a meta-analysis of the literature--part 1: comparison of traditional root-end surgery and endodontic microsurgery. *J Endod* 2010;36:1757-1765.  
[PUBMED](#) | [CROSSREF](#)
4. Kim S, Kratchman S. Modern endodontic surgery concepts and practice: a review. *J Endod* 2006;32:601-623.  
[PUBMED](#) | [CROSSREF](#)
5. Song M, Kim SG, Lee SJ, Kim B, Kim E. Prognostic factors of clinical outcomes in endodontic microsurgery: a prospective study. *J Endod* 2013;39:1491-1497.  
[PUBMED](#) | [CROSSREF](#)
6. Zhou W, Zheng Q, Tan X, Song D, Zhang L, Huang D. Comparison of mineral trioxide aggregate and iRoot BP Plus Root Repair Material as root-end filling materials in endodontic microsurgery: a prospective randomized controlled study. *J Endod* 2017;43:1-6.  
[PUBMED](#) | [CROSSREF](#)
7. Kim S, Jung H, Kim S, Shin SJ, Kim E. The influence of an isthmus on the outcomes of surgically treated molars: a retrospective study. *J Endod* 2016;42:1029-1034.  
[PUBMED](#) | [CROSSREF](#)
8. von Arx T, Hänni S, Jensen SS. Correlation of bone defect dimensions with healing outcome one year after apical surgery. *J Endod* 2007;33:1044-1048.  
[PUBMED](#) | [CROSSREF](#)
9. Sisk AL, Hammer WB, Shelton DW, Joy ED Jr. Complications following removal of impacted third molars: the role of the experience of the surgeon. *J Oral Maxillofac Surg* 1986;44:855-859.  
[PUBMED](#) | [CROSSREF](#)
10. Pinsky HM, Champlébox G, Sarment DP. Periapical surgery using CAD/CAM guidance: preclinical results. *J Endod* 2007;33:148-151.  
[PUBMED](#) | [CROSSREF](#)



11. Strbac GD, Schnappauf A, Giannis K, Moritz A, Ulm C. Guided modern endodontic surgery: a novel approach for guided osteotomy and root resection. *J Endod* 2017;43:496-501.  
[PUBMED](#) | [CROSSREF](#)
12. Song M, Kim SG, Shin SJ, Kim HC, Kim E. The influence of bone tissue deficiency on the outcome of endodontic microsurgery: a prospective study. *J Endod* 2013;39:1341-1345.  
[PUBMED](#) | [CROSSREF](#)
13. Gutmann JL, Harrison JW. Posterior endodontic surgery: anatomical considerations and clinical techniques. *Int Endod J* 1985;18:8-34.  
[PUBMED](#) | [CROSSREF](#)
14. Capuzzi P, Montebugnoli L, Vaccaro MA. Extraction of impacted third molars. A longitudinal prospective study on factors that affect postoperative recovery. *Oral Surg Oral Med Oral Pathol* 1994;77:341-343.  
[PUBMED](#) | [CROSSREF](#)
15. Mora MA, Chenin DL, Arce RM. Software tools and surgical guides in dental-implant-guided surgery. *Dent Clin North Am* 2014;58:597-626.  
[PUBMED](#) | [CROSSREF](#)
16. Floratos S, Kim S. Modern endodontic microsurgery concepts: a clinical update. *Dent Clin North Am* 2017;61:81-91.  
[PUBMED](#) | [CROSSREF](#)
17. Blumenthal NM. A clinical comparison of collagen membranes with e-PTFE membranes in the treatment of human mandibular buccal class II furcation defects. *J Periodontol* 1993;64:925-933.  
[PUBMED](#) | [CROSSREF](#)
18. Seibert JS. Reconstruction of deformed, partially edentulous ridges, using full thickness onlay grafts. Part I. Technique and wound healing. *Compend Contin Educ Dent* 1983;4:437-453.  
[PUBMED](#)
19. Rasmusson L, Meredith N, Kahnberg KE, Sennerby L. Effects of barrier membranes on bone resorption and implant stability in onlay bone grafts. An experimental study. *Clin Oral Implants Res* 1999;10:267-277.  
[PUBMED](#) | [CROSSREF](#)